RASĀYAN *J. Chem.*
Vol. 19 | No. 1 | 89-97 | January-March | 2026
ISSN: 0974-1496 | e-ISSN: 0976-0083 | CODEN: RJCABP
http://www.rasayanjournal.com
http://www.rasayanjournal.co.in

KINETICS AND EQUILIBRIUM OF MICROWAVE CATALYTIC PYROLYSIS ON LOW-RANK COAL USING $Fe_2(SO_4)_3$-HZSM-5

K. Khairuddin[1,✉], R. Ruslan[1], N.K. Sumarni[1], M.F. Rizki[1], M. Mahfud[2], B. Sardi[3], and M.A. Muttaqii[4]

[1]Department of Chemistry, Tadulako University, Palu-94118, Indonesia

[2]Department of Chemical Engineering, Sepuluh Nopember Institute of Technology, Surabaya-60111, Indonesia

[3]Research Centre for Energy Materials, National Research and Innovation Agency, South Tangerang-15314, Indonesia

[4]Research Centre for Catalysis Chemistry, National Research and Innovation Agency, South Tangerang-15314, Indonesia

✉Corresponding author: kjunus25@gmail.com

ABSTRACT

Microwave Catalytic Pyrolysis (MCP) has emerged as an effective method for converting low-rank coal (LRC) into valuable energy resources. This study investigated the kinetics and thermodynamics of LRC pyrolysis using a dual catalyst system of $Fe_2(SO_4)_3$-HZSM-5 under optimised operating conditions. The Coats–Redfern integral method was utilised to ascertain the kinetic parameters, indicating that the reaction adhered to first-order kinetics with 10.1 kJ/mol as an activation energy, demonstrating the significant catalytic effect in reducing the energy barrier. Calculations were performed for thermodynamic values, such as enthalpy (ΔH), entropy (ΔS), and Gibbs free energy (ΔG). The negative ΔH and ΔS values indicated an exothermic process with reduced molecular randomness, while the positive ΔG value revealed that the reaction did not occur spontaneously under the studied temperatures. These findings confirm the catalytic efficiency in enhancing LRC conversion and provide important insights into the feasibility and mechanism of the reaction. The study highlights the potential of MCP as a clean and efficient technology for utilising low-grade coal.

Keywords: Activation Energy; Reaction Kinetics; Low-Rank Coal; Microwave Catalytic Pyrolysis; $Fe_2(SO_4)_3$-HZSM-5 Catalyst

RASĀYAN *J. Chem.*, Vol. 19, No.1, 2026

INTRODUCTION

Low-rank coal (LRC) constitutes more than half of Indonesia's national coal resources, yet its direct application remains marginal. This type of coal carries unfavourable features such as high inherent moisture, elevated oxygen content, and relatively low heating value, which reduce its efficiency as a fuel.[1] To increase its economic potential, upgrading strategies are required that both add value and widen its scope of use. Among various approaches, pyrolysis stands out as an essential thermochemical route, serving as the entry point for further coal conversion processes and aligning with cleaner utilisation strategies. Despite a large body of research on coal pyrolysis, the kinetic characteristics of LRC are still not fully clarified. Understanding the reaction pathways and kinetic descriptors is crucial to predicting how LRC behaves under different thermal regimes and to optimising its conversion performance.[2,3] Thermogravimetric analysis (TGA) serves as a crucial method for examining the weight-loss characteristics of coal when subjected to heating.[4,5] From TGA curves, models can be derived that approximate the decomposition stages and provide estimates of the kinetic triplet—mechanism function, activation energy, and frequency factor.[6] Earlier investigations relied heavily on isothermal experiments, which only captured coal behaviour under fixed conditions.[7] Later, non-isothermal methods became popular, offering broader insight into decomposition kinetics. These methods can be applied either

http://doi.org/10.31788/RJC.2026.1919496

through differential or integral forms of the rate equation.[8,9] Although several studies have attempted to use these models on coal samples, direct comparisons between different approaches, particularly for LRC, remain uncommon.[10,11] This study addresses that gap by applying three non-isothermal methods, one differential and two integral, to the pyrolysis of LRC. By analysing the same dataset across different models, the study identifies how the choice of method affects the resulting kinetic parameters. To the best of the authors' knowledge, such a comparative evaluation of non-isothermal kinetics in LRC pyrolysis has not yet been reported.

EXPERIMENTAL

Materials and Samples Preparation

Low-rank coal was obtained from the Bobong Formation. The coal sample was desulfurised using $Fe_2(SO_4)_3$ solution, while the HZSM-5 catalyst was activated through calcination. The mixture consisted of 150 grams of LRC, $Fe_2(SO_4)_3$ as many as 24,6%, and 1,0% HZSM-5. The pyrolysis process was carried out in a Microwave Pyrolysis (MP) system under optimal conditions: frequency 2,45 GHz, input power 525 W, temperature 620°C, and reaction time 105 minutes, using a particle size of 100 mesh. The resulting products—bio-oil, syngas, and char—were analysed by GC-MS, FTIR, XRD, and SEM-EDS. All operational parameters, optimum condition data, and product characterisation procedures were based on the optimisation and analysis results reported in 2025.[12]

Kinetic and Equilibrium Analysis

Thermodynamic analysis was performed to obtain equilibrium parameters such as ΔG, ΔH, and ΔS to assess the practicality and balance properties of the microwave-assisted catalytic pyrolysis method. A mathematical model was constructed from TGA data on LRC pyrolysis with a non-isothermal approach. Two methods were applied: (1) CP + catalyst + receptor based on TGA data, and (2) MP + catalyst + receptor based on laboratory experiments. The experimental data were collected by determining reaction times that provided maximum conversion under MP conditions with catalyst and receptor addition.[13] (A) As the factor of pre-exponential was considered to remain constant and does not depend on temperature, thereby rendering it is suitable for temperature-programmed pyrolysis kinetics.[14] If the sample mass changed from w_0 (gram) to w_t (gram) at time t, the following equation was utilised:

$$\propto = \frac{w_0 - w_t}{w_0 - w_\infty} = \frac{\Delta w}{\Delta w_f} \quad (1)$$

Where w_0 is a symbol for initial mass (gram), w_t is mass at time t (gram), and w_∞ is be final mass after pyrolysis (gram). Heating was conducted at a constant rate $\beta = \frac{dT}{dt}$. According to the Coats–Redfern model,[15] pyrolysis reactions were assumed to follow the nth-order reaction of n_{th}:

$$y = 1 - x^{n} \quad (2)$$

where for n = 1, the equation applies: n = 1, $f(\alpha) = 1 - \alpha$,

$$\ln \frac{-\ln 1-\propto}{T^2} = \ln \frac{AR}{\beta E}\left(1 - \frac{2RT}{E}\right) - \frac{E}{RT} \quad (3)$$

While for n ≠ 1, it applies: n ≠ 1, $f(\alpha) = (1-\alpha)^n$,

$$\ln \frac{1-(1-\alpha)^{1-n}}{T^2(1-n)} = \ln \frac{AR}{\beta E}\left(1 - \frac{2RT}{E}\right) - \frac{E}{RT} \quad (4)$$

When $\frac{E}{RT} >> 1$, $\left(1 - \frac{2RT}{E}\right) \approx 1$The initial term on the right side of the two equations presented is nearly constant. Consequently, the plot of $\ln\left(\frac{\frac{d\alpha}{dT}}{f(\alpha)}\right)$ against $\frac{1}{T}$ Yields a linear relationship. Activation energy, which is symbolised by (E), can be derived from the slope, while the factor of pre-exponential can be calculated with the help of the intercept. Furthermore, the reaction of pyrolysis can exhibit a reaction

order of n. Consequently, n is evaluated for linear correlation, while E and A are derived concurrently. Based on te way of calculating he kinec parameters for different heatingrates, we can knowthat the curve etween $\ln\left[\frac{-\ln(1-\alpha)}{T^2}\right]$ (n = 1) and $\ln\left[\frac{1-(1-\alpha)^{1-n}}{T^2(1-n)}\right]$ (n ≠ 1) versus $\frac{1}{T}$ can be concluded and ordered differently for n = 1, n = 2, dan n = 3.

RESULTS AND DISCUSSION

Kinetics of Low-Rank Coal Pyrolysis

The decomposition of LRC proceeds through a chain of thermal cracking reactions, which can be broadly separated into solid–gas interactions and gas-phase transformations. The first group includes drying, devolatilization, combustion, and gasification with CO_2 or steam, while the latter involves secondary conversions such as the shift of water–gas and oxidation of H_2, CO, and CH_4.[16] Generally, the classification of these reactions, together with their enthalpy data, was summarised in Table-1.

Table-1: Reactions in the Non-Isothermal Cracking Process of LRC[17]

No.	Reaction Name	Reaction		Reaction Heat (kJ/mol)
Primary Reaction (Heterogeneous Reaction)				
1	Drying	$LRC_{(s)}$	→ LRC $dry_{(s)} + H_2O_{(g)}$	+40
2	Pyrolisis	LRC $dry_{(s)}$	→ $Char_{(s)} + Volatile_{(g)}$	0
3	Burning of LRC	C $(Char)_{(s)} + O_{2(g)}$	→ $CO_{2(g)}$	-393
4	CO_2 Gasification (Boudouard)	C $(Char)_{(s)} + CO_{2(g)}$	→ $2CO_{(g)}$	+172
5	Steam gasification	C $(Char)_{(s)} + H_2O_{(g)}$	→ $CO_{(g)} + H_{2(g)}$	+131
6	Methanation	C $(Char)_{(s)} + 2H_{2(g)}$	→ $CH_{4(g)}$	-75
Secondary Reaction (Homogeneous Reaction)				
7	Water-gas shift	$CO_{(g)} + H_2O_{(g)}$	↔ $CO_{2(g)} + H_{2(g)}$	-41
8		$CO_{(g)} + 0{,}5O_{2(g)}$	→ $CO_{2(g)}$	-111
9	Gas phase oxidation	$H_{2(g)} + 0{,}5O_{2(g)}$	→ $H_2O_{(g)}$	-242
10		$CH_{4(g)} + 2O_{2(g)}$	→ $CO_{2(g)} + 2H_2O_{(g)}$	-802

As shown in Table-1, the early stages are dominated by heterogeneous reactions, beginning with moisture release and volatile evolution, followed by the generation of solid char. With increasing temperature, secondary gas-phase reactions become more pronounced, supplying additional CO and H_2. The enthalpy distribution demonstrates that several reactions require external heat input, whereas others liberate energy, thus creating a dynamic thermal balance during the overall pyrolysis process. Beyond these fundamental steps, additional transformations involving decomposition, combustion, and gasification are also observed, as presented in Table-2.18. These reactions contribute to the conversion of char and volatiles into gaseous products such as H_2, CO, CH_4, and CO_2.

Table-2: List of Reactions Occurring in the Processes of Pyrolysis, Decomposition, Combustion, and Gasification[18]

No. Reaction	Chemical Reaction	
	Pyrolysis Process:	
1	Coal	→ Char + CH_4 + C_6H_6 + CO + CO_2 + H_2 + H_2O + H_2S + N_2
	Decomposition Process:	
2	Char	→ C + O_2 + H_2 + N_2 + S + Ash
	Combustion Process:	
3	$7{,}5O_2 + C_6H_6$	→ $3H_2O + 6CO_2$
4	$0{,}5O_2 + H_2$	→ H_2O
5	$0{,}5O_2 + CO$	→ CO_2
6	$2O_2 + CH_4$	→ $2H_2O + CO_2$

	Gasification Process	
7	$C + O_2$	$\rightarrow CO_2$
8	$C + 0{,}5O_2$	$\rightarrow CO$
9	$C + H_2O$	$\rightarrow CO + H_2$
10	$C + CO_2$	$\rightarrow 2CO$
11	$C + 2H_2$	$\rightarrow CH_4$
12	$H_2 + S$	$\rightarrow H_2S$
13	$0{,}5O_2 + H_2$	$\rightarrow H_2O$
14	$0{,}5O_2 + CO$	$\rightarrow C_2O$
15	$2O_2 + CH_4$	$\rightarrow 2H_2O + CO_2$
16	$H_2O + CO$	$\rightarrow CO_2 + H_2$
17	$H_2O + CH_4$	$\rightarrow 3H_2 + CO$

The presence of catalytic materials in contact with coal influences both the selectivity and the energy requirements of these reactions. Taken together, the reactions in Table-1 and Table-2 outline the essential kinetic framework that governs LRC pyrolysis, providing the basis for subsequent modelling and simulation efforts.

Thermogravimetric Analysis (TGA) Data

Thermogravimetric analysis (TGA) using the CP + $Fe_2(SO_4)_3$ + HZSM-5 method was conducted to determine the mass changes and thermal properties of LRC. The temperature range was established between 25°C and 1.000°C while maintaining a controlled flow of nitrogen gas. Fig.-1 illustrates the findings from the TGA analysis. The thermal stages that occurred during the pyrolysis and gasification of LRC were illustrated in Fig.-1. The TGA procedure began by mixing LRC, catalyst, and receptor in a defined ratio, then placing the mixture into a heated container. The sample was heated, and the degradation of LRC was observed. The initial stage of macromolecular degradation was drying, characterised by the intensity of water evaporation. Evaporation started with the release of external unbound moisture, followed by the evaporation of internal moisture in a quasi-stationary mode. The drying rate began to decrease upon reaching the critical moisture content. After drying, the next stage, primary pyrolysis, was characterised by the release of easily volatile pyrolytic substances. The formation of these primary volatiles resulted from the thermal cleavage of chemical bonds in LRC, including permanent gases (CO_2 , CO, H_2), volatile organic compounds (aliphatic and aromatic), and water. At this stage, a solid residue (char) rich in non-volatile carbon was formed, containing a significant portion of the original LRC mineral content. In general, the primary pyrolysis stage was completed around 500°C. As the temperature increased, part of the primary volatiles participated in various secondary pyrolysis reactions (500–700°C) and gasification processes (700–1,000°C).

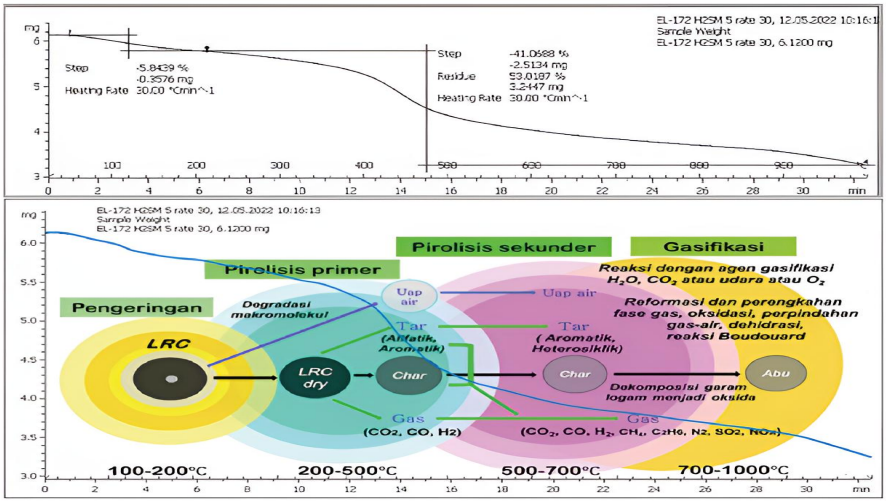

Fig.-1: TGA Analysis of LRC using the CP + $Fe_2(SO_4)_3$ + HZSM-5 Method

The TGA results of LRC using the CP + $Fe_2(SO_4)_3$ + HZSM-5 method showed multi-stage decomposition without intermediate product stability. The heating rate applied in the CP + $Fe_2(SO_4)_3$ + HZSM-5 method was 30°C/min, which included multi-stage decomposition with medium stability.[19] Figure-1 presents the TGA results of LRC treated with CP + $Fe_2(SO_4)_3$ + HZSM-5, showing that heating at 475°C for 15 minutes produced 53.02% solid residue (char). This result suggested that 46.98% of the volatile matter in LRC had undergone drying, primary pyrolysis, secondary pyrolysis, and gasification reactions. Considering that the difference in the amount of solid residue (char) due to the catalyst was not significant, it was concluded that the variation in residue mass was primarily due to the stability of the calcined catalyst and the direct contact between the catalyst-receptor system and the LRC. A more intricate model, known as the non-isothermal method, was employed to simulate the kinetics of LRC during thermal cracking.[19] The non-isothermal approach is classified into derivative and integral techniques based on the structure of the kinetic equations.[20] A significant number of studies have concentrated on utilising a singular non-isothermal kinetic model to investigate the thermal cracking behaviour of coal. [21, 22] The constant heating rate (β) derived from TGA data under non-isothermal conditions during the pyrolysis process was presented in Fig.-2.

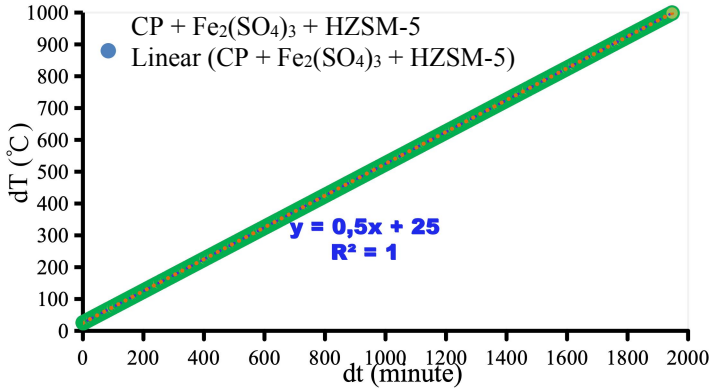

Fig.-2: The Heating Flow Rate of LRC Under Non-Isothermal Conditions using the CP + $Fe_2(SO_4)_3$ + HZSM-5 Method

Figure-2 showed the heating rate (β) of LRC under non-isothermal conditions using the CP + $Fe_2(SO_4)_3$ + HZSM-5 method was obtained as 0.5 °C/s (30 °C/min) with the regression equation (dT) = 0.5 (dt) + 25 and a coefficient of determination (R^2) = 1. Meanwhile, the determination of reaction order (n), apparent activation energy ($\frac{Ea}{R}$And the pre-exponential constant (A) was made by assuming the reaction order formed a linear line (y = axe + b) with an R value approaching 1,00. Thus, the reaction order value from the TGA data on the pyrolysis process occurring under non-isothermal conditions was shown in Fig.-3.

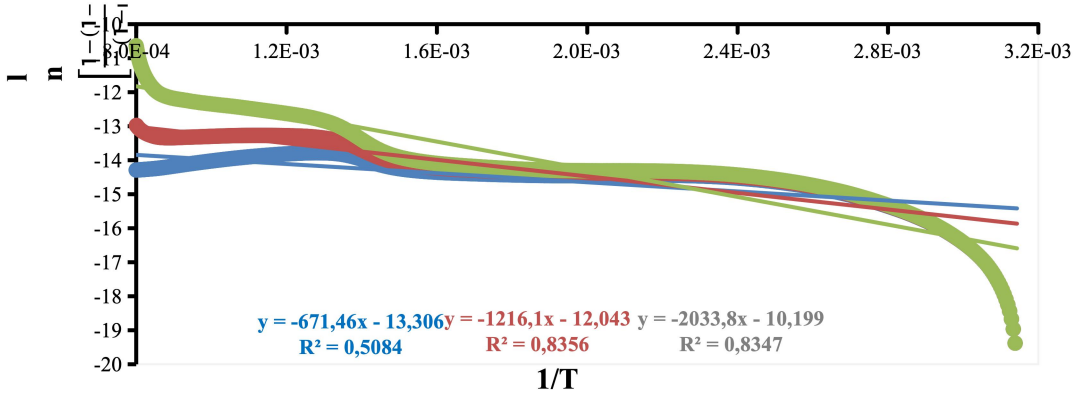

Fig.-3: Graph of Predicted Reaction Order (n): CP + $Fe_2(SO_4)_3$ + HZSM-5

The reaction order prediction graph (n) showed that the reaction order with a coefficient of determination (R^2) close to 1.00 could be determined. The best reaction order (n) for the heating rate of LRC from TGA data under non-isothermal conditions using the TGA + CP + $Fe_2(SO_4)_3$ + HZSM-5 method was order 1, with the regression equation (y) = -1216.1x – 12.043 and R^2 = 0.8356. The reaction mechanism can be defined by f(α) in relation to kinetic factors such as E and A. The reaction kinetics variables on the LRC from TGA data under non-isothermal conditions using the TGA + CP + $Fe_2(SO_4)_3$ + HZSM-5 method are shown in Table-3a and Table-3b.

Table-3a: Kinetic Parameters from Non-Isothermal TGA

Determination Method	Temp. (℃)	Heating Rate (℃/minute)	Reaction Order	Activation Energy (kJ/mol)	Pre-exponential Constant (1/s)	R^2
TGA + CP + $Fe_2(SO_4)_3$ + HZSM-5	25-1000	30	1	10,1	706.298,8	0,8356
TGA + CP	570-850	10	2	71,5	387,0	0,8870
TGA + CP	570-850	30	2	59,7	58,3	0,9410
TGA-Coal YN	520-660	30	2	71,80	1,4	0,9930
TGA-Coal XJ	510-700	30	2	101,1	3,6	0,9980

Table-3b: Reaction Equations and Literature Sources

Determination Method	Reaction Rate Equation	Description
TGA + CP + $Fe_2(SO_4)_3$ + HZSM-5	$k = 7{,}1.10^5 e^{-10{,}1/RT}$	The Results of This Research
TGA + CP	$k = 3{,}9.10^2 e^{-71{,}5/RT}$	(Xu, Zhang, & Wang, 2013)[23]
TGA + CP	$k = 5{,}8.10^1 e^{-59{,}7/RT}$	
TGA-Coal YN	$k = 0{,}1.10^1 e^{-71{,}8/RT}$	(Xu et al., 2015)[24]
TGA-Coal XJ	$k = 0{,}4.10^1 e^{-101/RT}$	

Data from Laboratory Experiments

Data from laboratory experiments using the MP + $Fe_2(SO_4)_3$ + HZSM-5 method, to determine the changes in mass and thermal properties of LRC with a process temperature interval of 550-650℃. The constant heating rate (β) value from the laboratory experimental data during the microwave pyrolysis process under non-isothermal conditions is shown in Fig.-4.

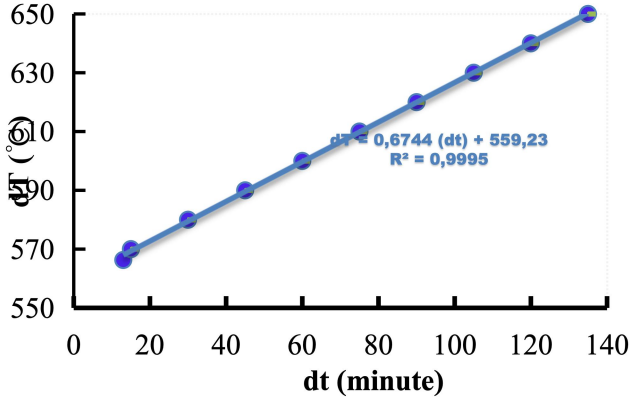

Fig.-4: The Heating Rate of LRC under Non-Isothermal Conditions using the MP + $Fe_2(SO_4)_3$ + HZSM-5 Method

Figure-4 showed that the heating rate (β) of LRC under non-isothermal conditions using the MP + HZSM-5 + $Fe_2(SO_4)_3$ method was obtained as 0,67℃/minute with the regression equation (dT) = 0,6744 (dt) + 559,23 and the coefficient of determination (R^2) = 0,9995. Meanwhile, the determination of the

reaction order (n), activation energy ($\frac{Ea}{R}$), and pre-exponential constant (A), assuming that the reaction order formed a linear line (y = axe + b) with an R value approaching 1,00. Thus, the reaction order value from the laboratory experimental data on the pyrolysis process occurring under non-isothermal conditions was shown in Fig.-5.

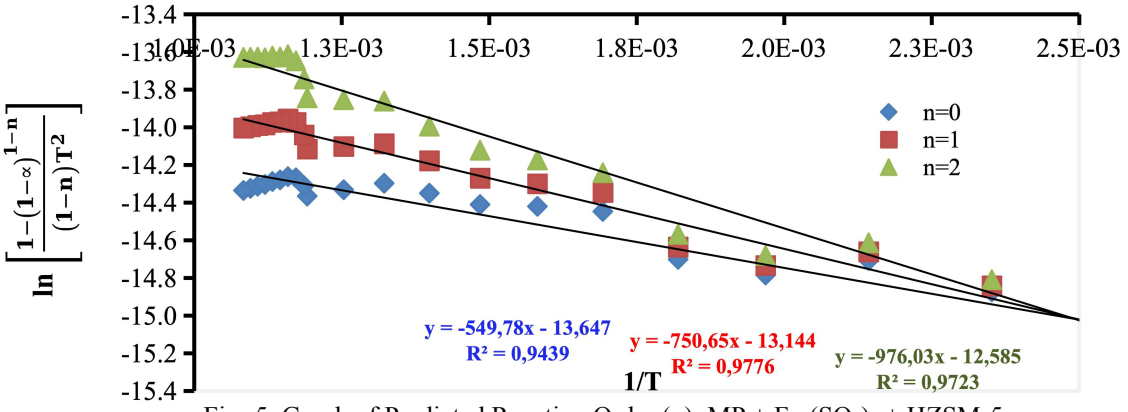

Fig.-5: Graph of Predicted Reaction Order (n): MP + $Fe_2(SO_4)_3$ + HZSM-5

From the reaction order prediction graph (n), the reaction order with a coefficient of determination (R^2) close to 1,00 could be determined. The best reaction order (n) for the heating rate of LRC from laboratory experimental data under non-isothermal conditions using the MP + $Fe_2(SO_4)_3$ + HZSM-5 method was order 1 with the regression equation (y) = -549.78x – 13.647 and R^2 = 0,9439. The reaction mechanism can be defined by f(α) in relation to kinetic factors such as E and A. The reaction kinetics variables in the LRC from laboratory experimental data under non-isothermal conditions using the MP + $Fe_2(SO_4)_3$ + HZSM-5 method are shown in Table-4a and Table-4b.

Table-4a: Reaction Kinetics Variables from Laboratory Experimental Data Under Non-Isothermal Conditions

Determination Method	Temp. (℃)	Heating Rate (℃/minute)	Reaction Order	Activation Energy (kJ/mol)	Pre-exponential Constant (1/s)	R^2
MP + $Fe_2(SO_4)_3$ + HZSM-5	550-650	1	1	6,2	4.310.925	0,9439
General Integral, SJC	350-650	5	1	223,7	$1,2.10^{14}$	0,9997
General Integral, WJG	350-650	5	1	217,0	$9,6.10^{12}$	0,9940
MacCallum-Tanner, SJC	350-650	20	1	158,0	$1,2.10^{9}$	0,9963
MacCallum-Tanner, WJG	350-650	20	1	192,4	$1,6.10^{11}$	0,9891

Table-4b: Reaction Equations and Literature Sources

Determination Method	Reaction Rate Equation	Description
MP + $Fe_2(SO_4)_3$ + HZSM-5	$k = 4,3.10^{6}e^{-6,2/RT}$	The results of this research
General Integral, SJC	$k = 1,2.10^{14}e^{-224/RT}$	(Zhang et al., 2019)[25]
General Integral, WJG	$k = 9,6.10^{12}e^{-217/RT}$	
MacCallum-Tanner, SJC	$k = 1,2.10^{9}e^{-158/RT}$	
MacCallum-Tanner, WJG	$k = 1,6.10^{11}e^{-192/RT}$	

CONCLUSION

The application of microwave-assisted catalytic pyrolysis (MCP) using the $Fe_2(SO_4)_3$-HZSM-5 catalyst system demonstrated significant potential in enhancing the conversion of low-rank coal (LRC) into high-value bio-oil and gas products. Although the operating parameters had been optimised in previous

research, this study specifically evaluated the reaction kinetics and thermodynamic equilibrium characteristics using the integral Coats–Redfern method. The analysis revealed that pyrolysis followed first-order kinetics with an activation energy of 10,1 kJ/mol, evidencing catalytic promotion through a reduced energy barrier. Thermodynamic assessment showed negative ΔH and ΔS values, confirming the exothermic nature of the process and a decrease in system disorder, while the positive ΔG value indicated that the reaction did not proceed spontaneously within the studied temperature range. These findings confirm the effectiveness of the catalytic system in accelerating the reaction and provide deeper insight into the underlying mechanisms. Moreover, the presence of $Fe_2(SO_4)_3$ as a sulfur receptor in combination with HZSM-5 played a crucial role in improving cracking selectivity while potentially reducing sulfur emissions. Overall, this process offers a practical and cleaner route for converting abundant low-value coal resources into sustainable energy products. Further investigations are recommended to assess catalyst stability under cyclic usage, evaluate technical and economic feasibility for scale-up, and explore process integration with biomass to improve product quality and enhance sustainability.

ACKNOWLEDGMENTS

The authors express their sincere gratitude for the support provided by the Faculty of Mathematics and Natural Sciences at Tadulako University, the Department of Chemical Engineering at Sepuluh Nopember Institute of Technology, and the Research Centre for Energy Materials at the National Research and Innovation Agency of Indonesia.

CONFLICT OF INTERESTS

The authors declare that there is no conflict of interest has been identified in relation to this study.

AUTHOR CONTRIBUTIONS

The present work is related to *SDG-7: Affordable and Clean Energy.* All the authors contributed significantly to this manuscript, participated in reviewing/editing and approved the final draft for publication. The research profile of the authors can be verified from their ORCID ids, given below:

K. Khairuddin https://orcid.org/0000-0002-5093-0869
R. Ruslan https://orcid.org/0000-0001-7249-5573
N.K. Sumarni https://orcid.org/0000-0003-4457-4404
M.F. Rizki https://orcid.org/0009-0000-4322-626X
M. Mahfud https://orcid.org/0000-0001-7740-9670
B. Sardi http://orchid.org/0000-0001-9555-0301
M.A. Muttaqii https://orcid.org/0000-0001-5000-3478

Cite this article as: K. Khairuddin *et al.*, *Rasayan J. Chem.*, 19(1), 89-97(2026), https://doi.org/10.31788/RJC.2026.1919496

REFERENCES

1. H. Saputro, L. Fitriana, A. Purwanto, R. Muslim, F.A. Munir, W.C. Wang, *Cleaner Engineering and Technology*, **21**, 100772(2024), https://doi.org/10.1016/j.clet.2024.100772.
2. D.F. Umar, Z. Zulfahmi, T. Suseno, S. Suganal, N. Madiutomo, L. Setiawan, E.A. Daranin, G. Gunawan, *Heliyon*, **9**, e22022(2023), https://doi.org/10.1016/j.heliyon.2023.e22022.
3. C. Manera, H.P. Fragoso, A.A. Agra, B.D. Flores, E. Osório, M. Godinho, A.C.F. Vilela, *Chemical Engineering Research and Design*, **196**, 427(2023), https://doi.org/10.1016/j.cherd.2023.06.063.
4. C. Ellison, V. Abdelsayed, M.W. Smith, *Fuel*, **354**, 129301(2023), https://doi.org/10.1016/j.fuel.2023.129301.
5. *Y. Ren, S. Gu, Z. Xu, Q. Wang, Journal of Analytical and Applied Pyrolysis*, **165**, 105559(2022), https://doi.org/10.1016/j.jaap.2022.105559.
6. Y.G. Wibowo, T. Taher, K. Khairurrijal, B.S. Ramadan, H. Safitri, S. Sudibyo, A.T. Yuliansyah,

H.T.B.M. Petrus, *Bioresource Technology Reports*, **25**, 101797(2024), https://doi.org/10.1016/j.biteb.2024.101797.
7. Y.N. Thaha, A. Ridhova, A.Y. Akbar, R. Hakim, Phiciato, N.I. Ciptasari, N. Darsono, M.N. Savitri, T.P. Elia, Muttaqin, *Diamond & Related Materials*, **142**, 110796(2024), https://doi.org/10.1016/j.diamond.2024.110796.
8. Y. Wang, X. Zhong, H. Zhao, J. Li, J. He, Y. Yang, L. Yan, *Journal of the Energy Institute*, **116**, 101752(2024), https://doi.org/10.1016/j.joei.2024.101752.
9. L. Wu, Y. Guan, C. Li, J. Zhou, T. Liu, G. Ye, Q. Zhang, Y. Song, R. Zhu, *Fuel*, **342**, 127860(2023), https://doi.org/10.1016/j.fuel.2023.127860.
10. X. Bai, A. Abedin, A.S.L. Gowda, V. Abdelsayed, P. Muley, *Fuel*, **372**, 132284(2024), https://doi.org/10.1016/j.fuel.2024.132284.
11. J. Zhu, F. Li, H. Wang, Z. Yang, H. Chen, H. Zhu, *Fuel*, **371(A)**, 131925(2024), https://doi.org/10.1016/j.fuel.2024.131925.
12. R. Ruslan, B. Sardi, K. Khairuddin, N. K. Sumarni, W. Tiro, Z. P. Magfira, N. Ainun and M. Mahfud, *Journal of the Energy Institute*, **119**, 101942(2025), https://doi.org/10.1016/j.joei.2024.101942.
13. Y. Xu, Y. Zhang, Y. Wang, *Reaction Kinetics, Mechanisms, and Catalysis,* **110**, 225(2013), https://doi.org/10.1007/s11144-013-0586-x.
14. S. Duzyol, C. Sensogut, *Journal of Combustion,* **2018**, 1(2018), https://doi.org/10.1155/2018/1761023.
15. Z. Feng, Z. Bai, H. Zheng, Z. Guo, L. Kong, J. Bai, W. Li, *Journal of Analytical and Applied Pyrolysis*, **145**, 1(2020), https://doi.org/10.1016/j.jaap.2019.104742.
16. S. Lyu, T. Cao, L. Zhang, J. Liu, G. Li, X. Ren, *International Journal of Energy Research*, **44(4)** 2652**(**2020), https://doi.org/10.1002/er.5011.
17. I. Ahmad, A. Ayub, N. Mohammad, M. Kano, *Sensors*, **19(7)**, 1(2019), https://doi.org/10.3390/s19071626.
18. K. Khairuddin, M.A. Ridhawansa, R. Ruslan, B. Sardi, *Cleaner Waste Systems*, **10**, 100225(2025), https://doi.org/10.1016/j.clwas.2025.100225.
19. M. Mahfud, A.H. Ramadhana, N.A. Novita, F. Kurniawansyah, B. Sardi, M.Mirzan, L. Mahmudin, A.A. Ali, N. Indrawan, *Energy*, **341**, 134309(2025), https://doi.org/10.1016/j.energy.2024.134309.
20. B. Sardi, I. Uno, F.A. Marhum, A.A. Akbar, T. Arief, M. Arif, A. Altway, M. Mahfud, *International Journal of Hydrogen Energy*, **49**, 203(2024), https://doi.org/10.1016/j.ijhydene.2023.07.217.
21. G. Wang, Y. Wang, J. Lv, Y. Wu, L. Jin, Y. Li, H. Yang, B. Hou, H. Hu, *Journal of the Energy Institute*, **104,** 1(2022), https://doi.org/10.1016/j.joei.2022.06.009.
22. X. Chen, Y. Ren, G. Qu, Z. Wang, Y. Yang, P. Ning, *Inorganic Chemistry Communications*, **157**, 111298(2023), https://doi.org/10.1016/j.inoche.2023.111298.
23. B. Sardi, I. Uno, F. Pasila, A. Altway, M. Mahfud, *FirePhysChem,* **3**, 106(2023), https://doi.org/10.1016/j.fpc.2023.02.002.
24. Y. Xu, Y. Zhang, Y. Wang, *Reaction Kinetics*, *Mechanisms and Catalysis*, **110(1)**, 225(2013), https://doi.org/10.1007/s11144-013-0586-x.
25. Y. Xu, Y. Zhang, G. Zhang, Y. Guo, J. Zhang, G. Li, *Journal of Thermal Analysis and Calorimetry*, **122(2)**, 975(2015), https://doi.org/10.1007/s10973-015-4801-z.
26. Q. Zhang, M. Luo, L. Yan, A. Yang, X. Hui, *Journal of Chemistry*, **2019**, 1(2019), https://doi.org/10.1155/2019/9075862.

[RJC-9496/2025]